Research Article

Journal of Environmental Nanotechnology

Effect of Copper Inclusion in Zinc sulfide Thin Films for Photocatalytic Applications

T. Shobana[1], R. Sakthi Sudar Saravanan[1] and D. Kathirvel[2*]

[1]Deparment of Physics, Chikkanna Government Arts College, Tiruppur, TN, India
[2]Department of Physics, Government Arts College (Autonomous), Coimbatore, TN, India
Received: 08.03.2024 Accepted: 27.03.2024 Published: 30.03.2024
*kathirvelde@gmail.com

ABSTRACT

Transparent and well-adhered pure zinc sulfide (ZnS) and different concentrations of copper-doped zinc sulfide thin films were obtained on glass substrates by the Chemical bath deposition process. Zinc acetate, copper acetate and thiourea were employed as sources of Zn^{2+}, Cu^{2+} and S^{2-} ions, respectively; ammonia and hydrazine hydrate served as complexing agents for the preparation of pure zinc sulfide and different concentrations of copper-doped zinc sulfide thin films. By adjusting the ammonia concentration, the prepared solution pH was maintained at 11. The prepared samples were deposited at the rates of 60 and 90 minutes each, with the bath temperature being held at 80 °C. The structural, morphological and optical properties of the prepared films were characterized by XRD, FE-SEM and EDX, and the results were reported. The XRD patterns revealed that all thin films possess a polycrystalline cubic zinc blended structure and that the prepared pure and copper-doped ZnS thin films have good crystallinity; the crystallite sizes were less than 20 nm. From the FE-SEM spectra, it is understood that the pure and Cu-doped ZnS thin films were uniformly coated with spherical morphology. The surface morphology, optical characteristics and deposition mechanism were all obviously impacted by the ammonia concentration. Additionally, under UV light irradiation, the effect of the photocatalytic property of the prepared thin films with methylene blue dye was studied and the corresponding dye degradation graphs were reported.

Keywords: Pure and Cu-doped ZnS thin films; CBD method; XRD analysis; FE-SEM analysis; Optical analysis; Photocatalytic; Methylene blue.

INTRODUCTION

The last 20 years have seen a global surge in the interest in tackling environmental challenges because of how rapidly society and industry are growing (Wu *et al.* 2022). The accumulation of wastewater discharges and domestic sewage that contains organic pollutants such as pesticides, antibiotics, and phenols is a major issue (Chen *et al.* 2021). In the meantime, the ecosystem is impacted and human health is harmed by the production of the dyeing and printing industries (Xu *et al.* 2018). An adequate treatment of wastewater to reduce environmental toxicity before discharging is of paramount importance (Mahalingam *et al.* 2023). For reducing the pollutants present in wastewater, semiconductor-based thin films act as a catalyst in the photocatalysis process which is the most effective and promising method (Jubeer *et al.* 2023). ZnS, CdS, CuS, as well as other metal chalcogenides that have been produced as thin films on different substrates, have new features that make them suitable for light-emitting diodes, electroluminescent devices, flat panel displays, infrared windows, photovoltaic sensors, lasers, solar cells and dye degradation applications (Li *et al.* 2010; Yu *et al.* 2014; Dedova *et al.* 2014; Deepa *et al.* 2014; Anne *et al.* 2022; Jubeer *et al.* 2023). Mainly, ZnS is one of the II-VI group's most important n-type semiconductor compounds with a wide direct band gap energy (3.6 eV), a high refractive index (2.35) and a low absorption coefficient, when it is in the form of a thin film (Erken *et al.* 2017). ZnS thin film plays a crucial role with dopant materials such as copper, manganese and nickel. (Jeon and Kang 2002; Soni *et al.* 2009; Chandrasekar *et al.* 2013). It allows for the enhancement of desirable features including their structure, wavelength emission and bandgap energy (Rosado *et al.* 2016; Mosavi and Kafashan, 2019). There are many methods available today for growing and depositing pure and Cu-doped ZnS thin films including thermal evaporation, sol-gel, spray pyrolysis, sputtering and sequential ionic-layer adsorption reaction (SILAR) (Lipina *et al.* 2019). Among these, chemical bath deposition (CBD) (Shobana *et al.* 2022) plays a significant part in thin film deposition since it uses affordable and non-toxic materials; it has garnered a lot of research interest. Moreover, the characteristics of pure and Cu-doped ZnS thin films produced by chemical bath deposition are influenced by NH_3 concentration; hydrazine hydrate acts as a complexing agent (Nicolau *et al.* 1990; Doña and Herrero, 1994; Arenas *et al.* 1997; Vidal *et al.* 1999; Mane *et al.* 2000). The thin films produced by CBD technique are typically either amorphous or poorly crystalline (Cheng *et al.* 2003). It was therefore necessary to anneal the thin films at a high temperature to increase their crystallinity. In this work,

glass substrates were used to deposit transparent, well-adhered pure (ZnS) and Cu-doped zinc sulfide (ZnS:Cu) thin films. Then, the prepared thin films were characterized to study their structural, morphological and optical characteristics.

2. MATERIALS AND METHODS

2.1 Materials

All the reagents namely zinc acetate ($Zn(CH_3COO)_2$), copper acetate ($Cu(CH_3COO)_2)_2$, thiourea ($SC(NH_2)_2$), ammonia (NH_3) and hydrazine hydrate (N_2H_4) purchased from Merck, without any further purification, served as complexing agents for the preparation of pure and Cu-doped ZnS thin films. Deionized water was used in all of the cleaning and solutions preparation steps.

2.2 Experimental Work

Pure and Cu-doped ZnS thin films were formed on well-treated microscope glass slide substrates. The preparation of substrates is essential in the CBD technique. The substrate cleaning procedure included an overnight soak in chromic acid, followed by a rinse in distilled water and a 20-minute ultrasonic cleaning session using an equal volume of acetone and alcohol. To provide better adhesion and consistency of the prepared solution applied to the substrate, the glass substrates were lightly scraped prior to vertical immersion in the bath solution.

In a typical process for the synthesis of pure ZnS solution, 20 ml of 0.5 M zinc acetate, 80% hydrazine hydrate and 0.5 M thiourea were initially taken, then deionized water was added to make the solution up to 100 ml. Initially, hydrazine hydrate and zinc acetate solutions were made, combined, and thoroughly stirred until the solution was clear. The mixture was then given a good stir before the ammonia solution was added. 20 ml of thiourea solution was made simultaneously, and both solutions were slowly mixed while being stirred at room temperature to ensure a homogeneous combination. After that, while altering the ammonia solution, the pH of the solution was kept at 11. Once the solution is prepared, it should be transferred to a 100 ml beaker that has been meticulously cleaned and placed in a chemical bath that has been preheated to 80 °C. Without stirring, the perfectly cleaned substrate was immersed vertically in the deposition solution for 60 and 90 minutes (Z1 and Z2, respectively). The as-deposited thin films were then dried and cleaned with distilled water. The as-prepared thin films were homogeneous, smooth and had good substrate adhesion with the color of a white film.

For Cu-doped thin films, 0.05 mole of copper acetate is added to the parent ZnS stock solution. The 5 moles % Cu-doped ZnS thin films were prepared similarly (ZC1 and ZC2, respectively). Finally, as-deposited thin films were annealed at 400 °C.

Using X-ray diffraction (XRD), the physical and phase characteristics of the as-prepared thin films were examined. The morphological characteristics were examined using a Field emission scanning electron microscope (FE-SEM). The constituent components of pure and Cu-doped ZnS thin films were found using Electron dispersive spectroscopy (EDS); UV-Vis spectroscopy was used to investigate optical characteristics.

3. RESULTS AND DISCUSSION

3.1 XRD Studies

XRD patterns of pure and Cu-doped ZnS thin films are represented in Fig. 1. It can be seen that these XRD patterns have maximum intensity peaks at 2θ that correspond to the (200) and (220) crystallographic planes, respectively. This peak represents the cubic ZnS phase (ICDD PDF:65-1691) (Kumar *et al.* 2016). The planes mentioned above are those of polycrystalline cubic ZnS. Due to an increase in film thickness caused by an increase in molarity, the diffraction intensity rises, indicating more Bragg planes. It is evident that the Bragg's peaks increased with increasing time deposition rate, clearly suggesting an increase in crystallization. As per reports, this behavior is noticeably a standard routine (Kumar *et al.* 2016). The average crystalline sizes (D) of as-prepared pure ZnS and Cu-doped ZnS thin films with different deposition times, estimated using Scherer's equation, were given in Table 1 (Hassan *et al.* 2019; Jrad *et al.* 2021):

$$D = \frac{0.9\lambda}{\beta \cos\theta}$$

where, λ is the wavelength of the X-ray, β is FWHM-full width and half maximum.

From Table 1, it is evident that with the incorporation of a dopant into the parent ZnS lattice, the crystallite size slightly increased. Moreover, the crystallite size of the thin films (pure and doped ZnS) increased with the increase in deposition time from 60 to 90 minutes.

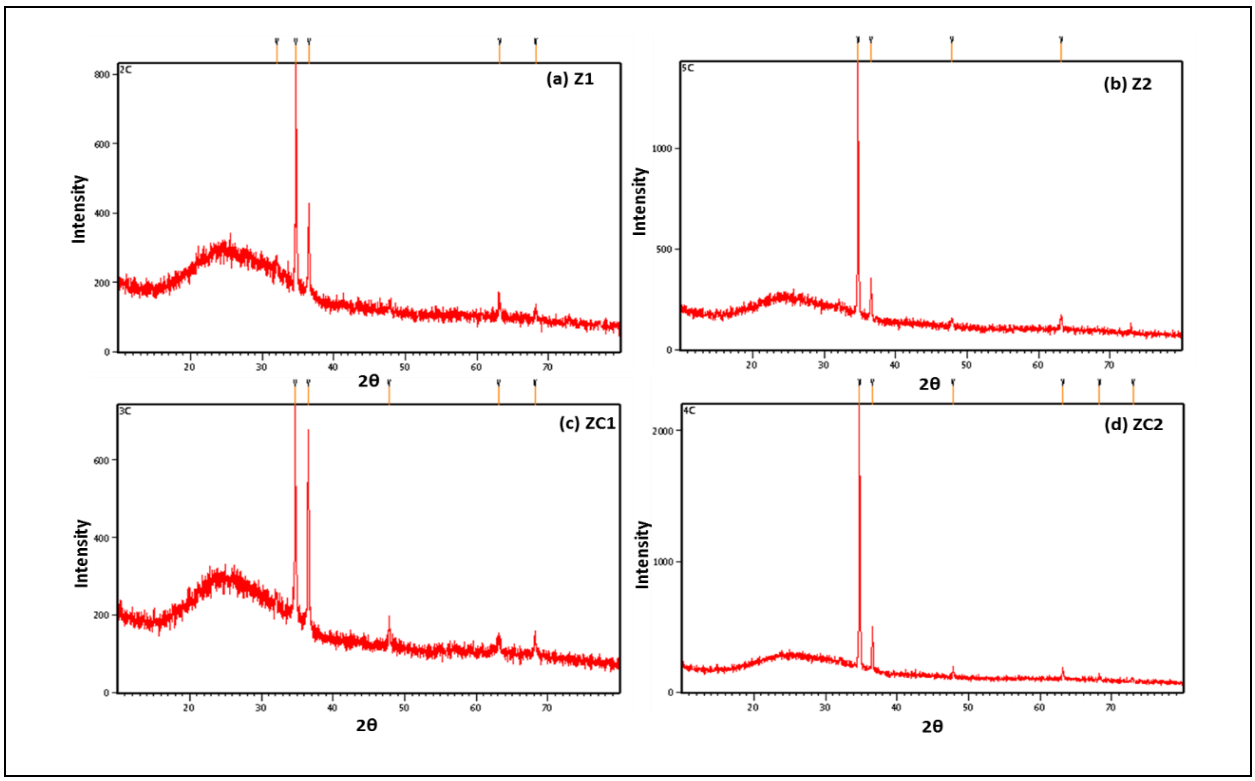

Fig. 1: XRD patterns of Pure and Cu-doped ZnS thin films

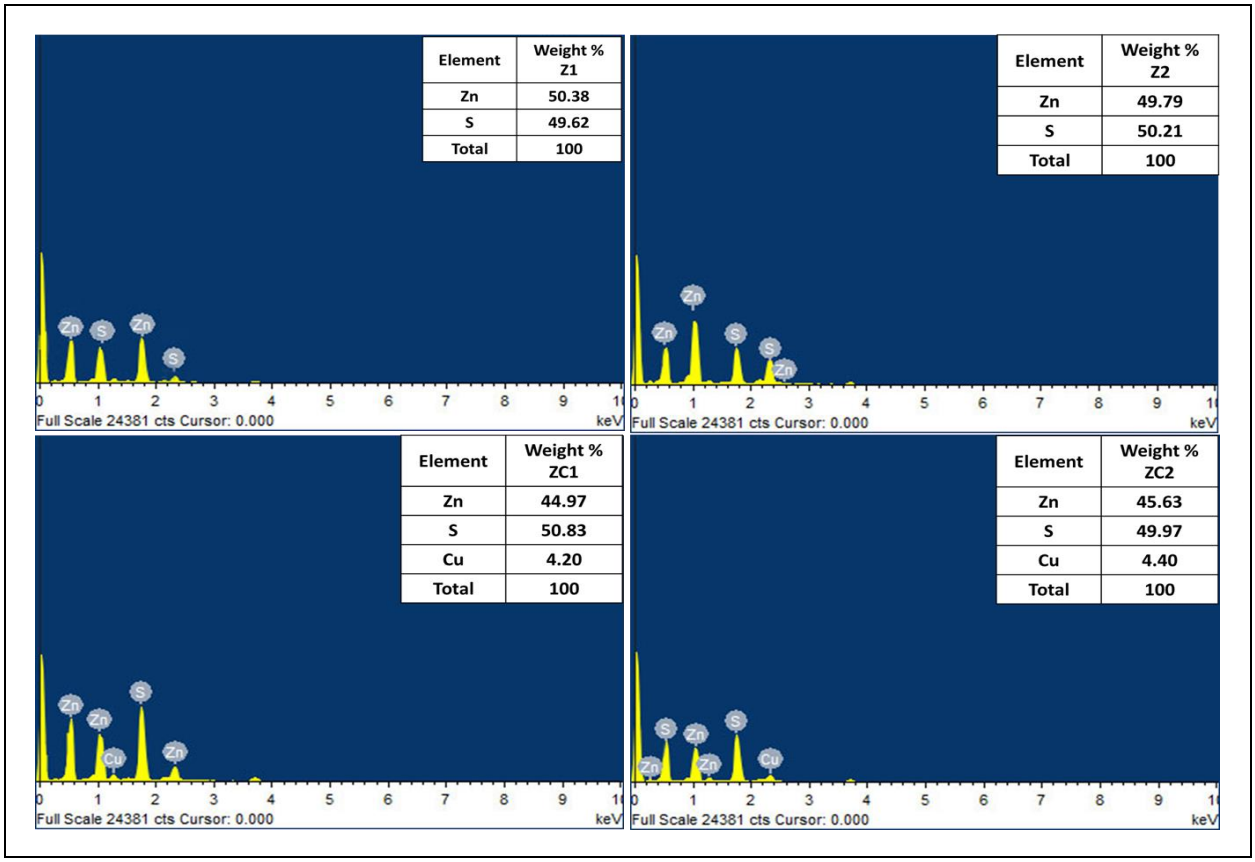

Fig. 2: Elemental Composition of Pure and Cu-doped thin films from EDX analysis

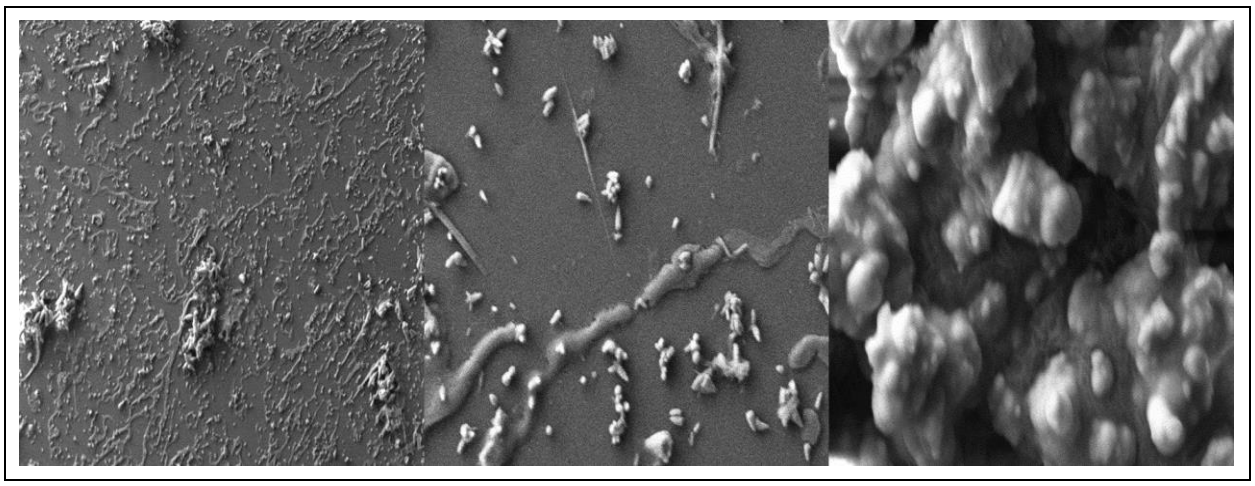

Fig. 3: SEM images of Pure and Cu-doped ZnS thin films

3.2 EDX Analysis

Fig. 2 displays the EDX spectra of the Cu-doped ZnS thin films formed at various deposition time rates at 60 and 90 minutes. All the thin film layers showed the presence of zinc and sulfur. The formation of pure ZnS thin films is evidenced by the existence of Zn and S peaks. The creation of the Cu-doped ZnS thin films is shown by the presence of Zn, S, and Cu-related peaks. Additionally, it demonstrated how closely the deposited films matched their stoichiometry (Göde *et al.* 2007). The data for each element's atomic percentages from the EDX analysis is also shown in Fig. 2. It should be noticed that the zinc atomic percentage in the thin films is lower than the sulfur atomic percentage. It can be observed that the real Zn:S atomic ratio decreases as deposition time increases while the Cu:Zn molar ratio in the deposition solution increases (Yuan *et al.* 2014); in other words, as the Cu dopant's thin film deposition time grew, so did the quantity of zinc vacancy states (ZnS) in the host lattice (Rosado *et al.* 2016).

3.3. Morphological Investigations (FE-SEM)

The morphological images of the pure and Cu-doped ZnS thin films obtained using FE-SEM are shown in Fig. 3. It revealed the surface characteristics of isolated big grains deposited on a surface formed with very small grains. The grain size increased with the increase in depositing time. Cu-doped ZnS thin film grain size also increased; the small grains combined with the big ones increased their size. Thus, it shows the combination between them to form clusters (Rosado *et al.* 2016). As a result, it is proven that sudden changes in surface morphology are closely connected to the amount of Cu doping (Ortíz *et al.* 2014).

3.4 Optical Properties

The optical absorption of pure and Cu-doped ZnS as-deposited thin films was examined using wavelengths ranging from 250 to 900 nm. Strong absorption peaks were absorbed between 300 and 350 nm for both pure and Cu-doped ZnS thin films, respectively. By measuring the thickness of the prepared thin films and the absorption coefficient (α), which is estimated from absorbance studies, it is possible to identify the band gap value of pure and doped materials. The following equation uses the absorption coefficient (α) to compute the band gap of the as-deposited ZnS thin film (Sathishkumar *et al.* 2019).

$$\alpha = \frac{2.303 * A}{d}$$

where, d is the film thickness and A is the absorbance of the film. Furthermore, using Taucs plots (Shaili *et al.* 2021), the optical energy band gap of as-deposited ZnS thin films was predicted. It has a relationship with photon energy and absorption coefficient:

$$(\alpha h\nu)^2 = A(h\nu - E_g)$$

where, A is the constant which is related to the effective mass associated with the bands, α is the absorption coefficient, h is Planck's constant (6.626 x 10^{-34} Js) and ν is the frequency in Hz. Fig. 4 shows the plots of absorbance as a function of the energy gap. The band gap values of the undoped and Cu-doped ZnS thin films were determined and presented in Table 1.

Table 1. Summary of crystallite sizes and optical bandgap of prepared thin films

Sample Code	Crystallite size (nm)	Energy gap (eV)
Z1	15.4	3.76
Z2	16.6	3.79
ZC1	15.9	3.62
ZC2	17.3	3.68

From the table, it was inferred that the energy gap of the pure and Cu-doped ZnS thin films increased when the deposition time was lengthened; the prepared thin films' absorbance was found to decrease.

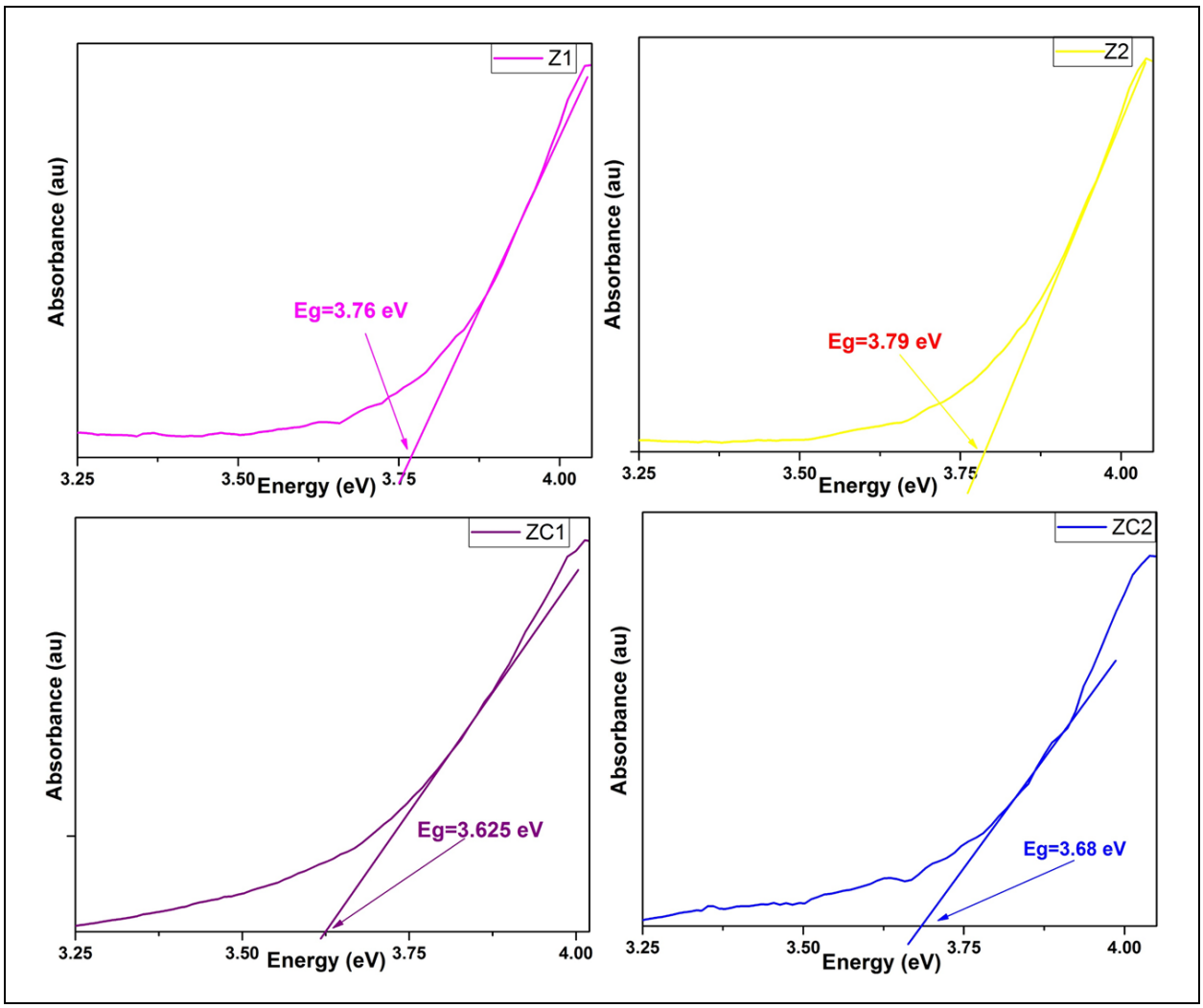

Fig. 4: Optical properties of Pure and Cu-doped ZnS thin films

3.5 Photocatalytic Activity of ZnS Thin Film Mechanism

A 15 W UV irradiation lamp was used to carry out the dye degradation experiment and there was a 5 cm gap maintained between the light and the liquid surface (methylene blue dye). UV light releases the photon energy (E = 4.89 eV) which helps the electrons free from the valance band of the ZnS thin film. The freed electrons (called photogenerated electrons) jump to the conduction band and subsequently form holes (called photogenerated holes) in the ZnS thin film. Therefore, the photogenerated electrons and holes can recombine in two ways to produce the superoxide radicals ($^{\bullet}O_2^-$) and hydroxyl radicals ($^{\bullet}OH^-$), respectively; the mechanism of the photocatalytic reaction can by described (Lee and Wu, 2017; Kaur *et al.* 2021) as follows:

$$ZnS + hv \rightarrow e^- + h^+$$

$$H_2O \rightarrow {}^{\bullet}OH + h^+$$

$$OH^- + h^+ \rightarrow {}^{\bullet}OH^-$$

$$O_2 + e^- \rightarrow {}^{\bullet}O_2^-$$

$$MB + {}^{\bullet}OH^- \rightarrow Products\ (CO_2 + H_2O) + Inorganic\ acids$$

$$MB + {}^{\bullet}O_2^- \rightarrow Products\ (CO_2 + H_2O) + Inorganic\ acids$$

A schematic representation of the ZnS thin film's photocatalytic activity using methylene blue (MB) dye was shown in Fig. 5.

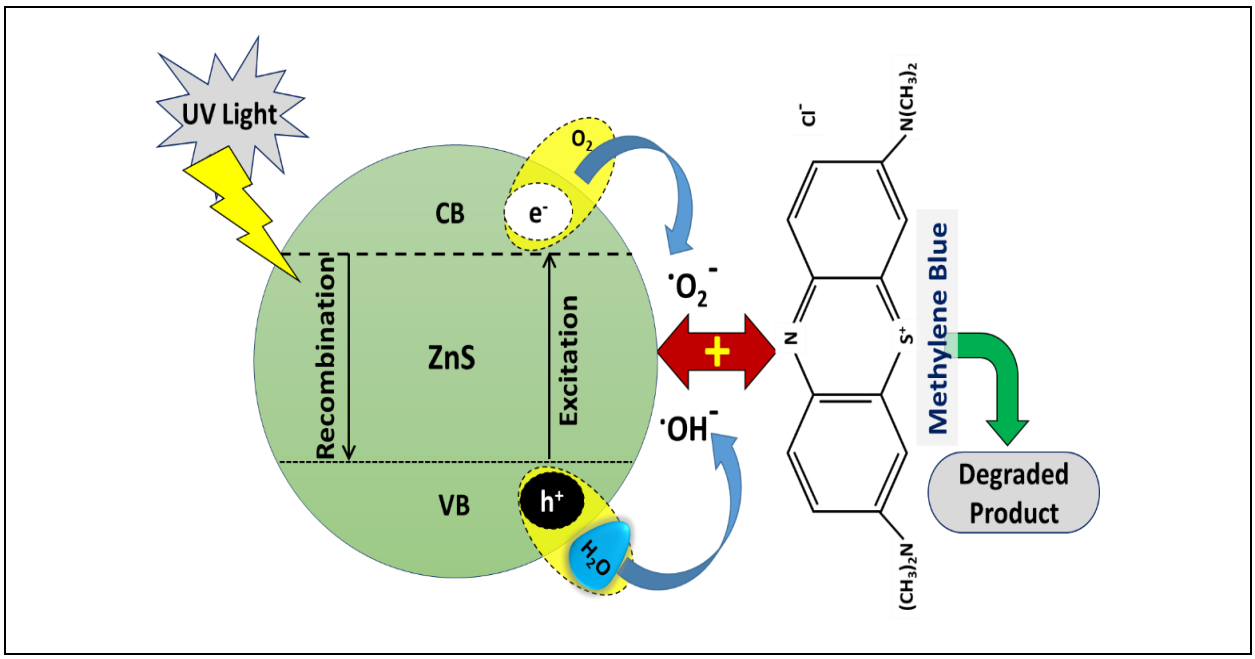

Fig. 5: A schematic diagram of Photocatalytic degradation for MB dye

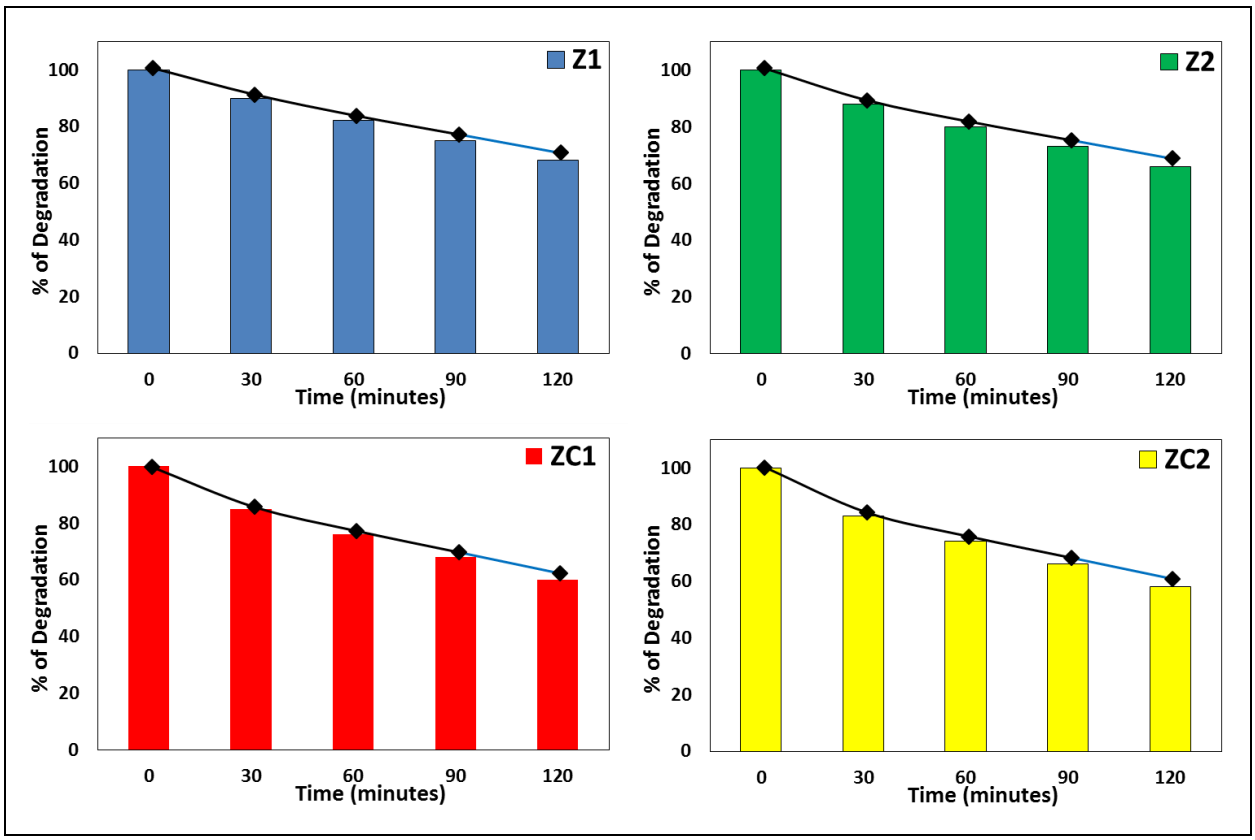

Fig. 6: Efficiency of Photocatalytic degradation of MB dye

100 ml of an aqueous solution containing 10 ppm of MB dye was first agitated for 30 minutes to attain equilibrium in the dark condition, after which as-prepared ZnS thin film was added as a catalyst. At specified time intervals (0, 30, 60 and 120 min), 3 ml degraded solutions were analyzed using a UV-Vis spectrophotometer and the characteristic absorption peak of MB dye solution at 662 nm was examined. The degradation efficiency (η) has been calculated (Ajibade *et al.* 2022) using the relation,

$$\eta(\%) = \left(\frac{C_0 - C_t}{C_0}\right) 100\%$$

where, C_0 represents initial concentration of MB dye and C_t represents the MB dye concentration of the photocatalytic process under UV light irradiation over the specified time. The calculated efficiency of the samples was graphically represented in Fig. 6 for the four samples and the comparison of efficiencies of the four samples was depicted in Fig. 7.

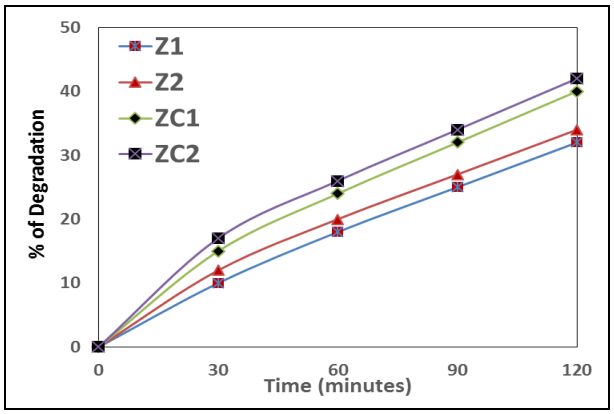

Fig. 7: Comparison of Efficiencies of the samples

Fig. 7 indicates that the prepared samples' efficiencies are nearly the same for both 60- and 90-minute thin film deposition times. After 120 minutes of the photocatalytic process of pure ZnS thin films serving as catalysts with MB dye, 32% and 34% of the efficiencies were obtained for the deposition rate of 60 and 90 minutes, respectively. Similarly, 40% and 42% efficiency were attained when using Cu-doped ZnS thin films as a catalyst with MB dye. It indicates that the percentage efficiency of the MB dye degradation process was not significantly affected by the deposition period; however, ZnS:Cu works as a better photocatalyst than pure ZnS thin films after 120 minutes. Furthermore, a notable decrease in dye degradation efficiency is observed with an increase in Cu concentration in ZnS thin films (Mehrabian and Esteki, 2017). According to Mehrabian and Esteki, the dopants produced ionized impurity scattering from interstitials and substitution acceptors, which in turn caused the carrier concentration to decrease (Mehrabian *et al.* 2017). In order to address the issue, un-doped and doped ZnS are employed as nanoparticles, which offer greater efficiency than thin films (Kaur *et al.* 2015). Additionally, the dopant material can create an alloy with the host material, which has significant effects on the pollutant removal process *via* photocatalysis (Chauhan *et al.* 2014).

4. CONCLUSION

In the present study, transparent and well-adhered pure and Cu-doped ZnS thin films were effectively deposited on glass substrates at the rates of 60 and 90 minutes each using a straightforward CBD procedure. The prepared films' structural, morphological and optical characteristics were examined and reported using various characterization techniques. It was inferred from the XRD results that the zinc structure was polycrystalline cubic in all thin films. The optical investigations of the pure and Cu-doped ZnS films suggested the applicability for semiconductor devices due to the low energy gap of the Cu-doped ZnS thin films. Photocatalytic degradation of MB using pure and Cu-doped ZnS thin films was performed under UV light irradiation at varying deposition times. The samples' efficiencies have been calculated and reported. It is evident that catalysts in the form of nanoparticles will receive a lot of attention in the future.

FUNDING

This research received no specific grant from any funding agency in the public, commercial, or not-for-profit sectors.

CONFLICTS OF INTEREST

The authors declare that there is no conflict of interest.

REFERENCE

Ajibade, P. A., Solomane, N. and Sikakane, B. M., Morphological studies and photocatalytic degradation of methylene blue by zinc sulfide nanoparticles, *Chalcogenide Lett.*, 19(6), 429–438 (2022). https://doi.org/10.15251/CL.2022.196.429

Anne, S. C. R., Prakash, I., Alex Arunmozhi, A., Chakravarty, S. and Leo R. A., Variation of sulfur concentration on the effective deposition of solution processed ZnS thin films for buffer layer in thin film solar cells, *Mater. Today Proc.*, 68, 356–362 (2022). https://doi.org/10.1016/j.matpr.2022.05.569

Arenas, O. L., Nair, M. T. S. and Nair, P. K., Chemical bath deposition of ZnS thin films and modification by air annealing, *Semicond. Sci. Technol.*, 12(10), 1323–1330 (1997). https://doi.org/10.1088/0268-1242/12/10/022

Chandrasekar, L. B., Raji, P., Chandramohan, R., Vijayalakshmi, R. and Devi, G., Shunmugasundram, P., Sindhu, P., Synthesis, Micro-Structural and Optical Properties of Cr Doped ZnS Nanoparticles Prepared by Chemical Precipitation Method, *J. Nanoelectron. Optoelectron.*, 8(4), 369–372 (2013). https://doi.org/10.1166/jno.2013.1481

Chauhan, R., Kumar, A. and Pal, C. R., Photocatalytic degradation of methylene blue with Cu doped ZnS nanoparticles, *J. Lumin.*, 145, 6–12 (2014). https://doi.org/10.1016/j.jlumin.2013.07.005

Chen, X., Memon, H. A., Wang, Y., Marriam, I. and Tebyetekerwa, M., Circular Economy and Sustainability of the Clothing and Textile Industry, *Mater. Circ. Econ.*, 3(1), 12 (2021). https://doi.org/ 10.1007/s42824-021-00026-2

Cheng, J., Fan, D., Wang, H., Liu, B., Zhang, Y. and Yan, H., Chemical bath deposition of crystalline ZnS thin films, *Semicond. Sci. Technol.*, 18(7), 676–679 (2003). https://doi.org/10.1088/0268-1242/18/7/313

Dedova, T., Krunks, M., Gromyko, I., Mikli, V., Sildos, I., Utt, K. and Unt, T., Effect of Zn:S molar ratio in solution on the properties of ZnS thin films and the formation of ZnS nanorods by spray pyrolysis, *Phys. status solidi.*, 211(2), 514–521 (2014). https://doi.org/ 10.1002/pssa.201300215

Deepa, K., Preetha, K. C., Murali, K. V., Dhanya, A. C., Ragina, A. J. and Remadevi, T. L., The effect of various complexing agents on the morphology and optoelectronic properties of chemically deposited ZnS thin films: A comparative study, *Optik (Stuttg).* 125(19), 5727–5732 (2014). https://doi.org/ 10.1016/j.ijleo.2014.06.028

Doña, J. M. and Herrero, J., Process and Film Characterization of Chemical-Bath-Deposited ZnS Thin Films, *J. Electrochem. Soc.*, 141(1), 205–210 (1994). https://doi.org/10.1149/1.2054685

Erken, O., Gunes, M. and Gumus, C., Synthesis of Mn-doped ZnS thin films by chemical bath deposition: Optical properties in the visible region, AIP Conf. Proc., 1833(1), 020093 (2017). https://doi.org/10.1063/1.4981741

Göde, F., Gümüş, C. and Zor, M., Investigations on the physical properties of the polycrystalline ZnS thin films deposited by the chemical bath deposition method, *J. Cryst. Growth*, 299(1), 136–141 (2007). https://doi.org/10.1016/j.jcrysgro.2006.10.266

Hassan, E. S., Mubarak, T. H., Chiad, S. S., Habubi, N. F., Khadayeir, A. A., Dawood, M. O., Al, B. I. A., Physical Properties of indium doped Cadmium sulfide thin films prepared by (SPT), *J. Phys. Conf. Ser.*, 1294(2), 022008 (2019). https://doi.org/10.1088/1742-6596/1294/2/022008

Jeon, H.-J., Kang, Y. S., Synthesis of ZnS:Mn 2+ Nanocrystals And Luminescence Properties Of Ldpe Film Containing ZnS:Mn 2+, *Int. J. Nanosci.*, 1, 495–499 (2002). https://doi.org/10.1142/S0219581X02000565

Jrad, A., Naouai, M., Abdallah, A., Ammar, S. and Turki, K., N., Doping ZnS films with cobalt: Structural, compositional, morphological, optical, electrical, magnetic and photocatalytic properties, *Phys. B Condens. Matter.*, 603, 412776 (2021). https://doi.org/10.1016/j.physb.2020.412776

Jubeer, E. M., Manthrammel, M. A., Subha, P. A., Shkir, M., Biju, K. P. and AlFaify, S. A., Defect engineering for enhanced optical and photocatalytic properties of ZnS nanoparticles synthesized by hydrothermal method, *Sci. Rep.*, 13(1), 16820 (2023). https://doi.org/10.1038/s41598-023-43735-1

Kaur, A., Kaur, B., Singh, K., Kumar, R. and Chand, S., Study of precursor-dependent CuS nanostructures: crystallographic, morphological, optical and photocatalytic activity, *Bull. Mater. Sci.*, 44(4), 268 (2021). https://doi.org/10.1007/s12034-021-02558-4

Kaur, J., Sharma, M., Pandey, O. P., Structural and optical studies of undoped and copper doped zinc sulfide nanoparticles for photocatalytic application, *Superlattices Microstruct.*, 77, 35–53 (2015). https://doi.org/10.1016/j.spmi.2014.10.032

Kumar, N., Purohit, L. P. and Goswami, Y. C., Spin coating of ZnS nanostructures on filter paper and their characterization, *Phys. E Low-dimensional Syst. Nanostructures*, 83, 333–338 (2016). doi: https://doi.org/10.1016/j.physe.2016.04.025

Lee, G. J., Wu, J. J., Recent developments in ZnS photocatalysts from synthesis to photocatalytic applications — A review, *Powder Technol.* 318, 8–22 (2017). https://doi.org/10.1016/j.powtec.2017.05.022

Li, Z. Q., Shi, J. H., Liu, Q. Q., Wang, Z. A., Sun, Z. and Huang, S. M., Effect of [Zn]/[S] ratios on the properties of chemical bath deposited zinc sulfide thin films, *Appl. Surf. Sci.*, 257(1), 122–126 (2010). https://doi.org/10.1016/j.apsusc.2010.06.047

Lipina, O. A., Gagarin, R. A., Maskaeva, L. N., Markov, V. F. and Voronin, V. I., Effect of copper doping on luminescent characteristics of chemically deposited ZnS thin films, AIP Conf. Proc., 2063(1), 040034 (2012). https://doi.org/10.1063/1.5087366

Mahalingam, S., Neelan, Y. D., Bakthavatchalam, S., Al-Humaid, L. A., Al- Dahmash, N. D., Santhanam, H., Yang, T.-Y., Hossain, N., Park, S. H. and Kim, J., Effective Visible-Light-Driven Photocatalytic Degradation of Harmful Antibiotics Using Reduced Graphene Oxide-Zinc Sulfide-Copper Sulfide Nanocomposites as a Catalyst, *ACS Omega*, 8(36), 32817–32827 (2023). https://doi.org/ 10.1021/acsomega.3c03883

Mane, R. S., Lokhande, C. D., Chemical deposition method for metal chalcogenide thin films, *Mater. Chem. Phys.*, 65(1), 1–31 (2000). https://doi.org/10.1016/S0254-0584(00)00217-0

Mehrabian, M. and Esteki, Z., Degradation of methylene blue by photocatalysis of copper assisted ZnS nanoparticle thin films, *Optik (Stuttg).*, 130, 1168–1172 (2017). https://doi.org/10.1016/j.ijleo.2016.11.137

Mosavi, S. M. and Kafashan, H., Physical properties of Cd-doped ZnS thin films, *Superlattices Microstruct.*, 126, 139–149 (2019). https://doi.org/10.1016/j.spmi.2018.12.002

Nicolau, Y. F., Dupuy, M. and Brunel, M., ZnS , CdS , and Zn1 − x Cd x S Thin Films Deposited by the Successive Ionic Layer Adsorption and Reaction Process, *J. Electrochem. Soc.*, 137(9), 2915–2924 (1990). https://doi.org/10.1149/1.2087099

Ortíz-Ramos, D. E., González, L. A. and Ramirez, B. R., p-Type transparent Cu doped ZnS thin films by the chemical bath deposition method, *Mater. Lett.* 124, 267–270 (2014). https://doi.org/10.1016/j.matlet.2014.03.082

Rosado, M. and Oliva, A. I., Chemical Bath Deposition of Zinc Sulfide Films Doped With Copper, *Mater. Manuf. Process.*, 31(11), 1454–1460 (2016). https://doi.org/10.1080/10426914.2016.1140185

Sathishkumar, M., Saroja, M. and Venkatachalam, M., Influence of (Cu, Al) doping concentration on the structural, optical and antimicrobial activity of ZnS thin films prepared by Sol-Gel dip coating techniques, *Optik (Stuttg).*, 182, 774–785 (2019). https://doi.org/10.1016/j.ijleo.2019.02.014

Shaili, H., Salmani, E. M. E. R., Beraich, M., Battal, W., Ouafi, M., Elhat, A., Rouchdi, M., Ez, Z. H., Hassanain, N. and Mzerd, A., Structural, electronic and optical properties of Cu-doped ZnS thin films deposited by the ultrasonic spray method- DFT study, *Opt. Quantum Electron.*, 53(6), 300 (2021). https://doi.org/10.1007/s11082-021-02934-8

Soni, H., Chawda, M., Bodas, D., Electrical and optical characteristics of Ni doped ZnS clusters, *Mater. Lett.*, 63(9–10), 767–769 (2009). https://doi.org/ 10.1016/j.matlet.2008.12.052

Shobana, T., Venkatesan, T. and Kathirvel, D., A Comprehensive Review on Zinc Sulfide Thin Film by Chemical Bath Deposition Techniques, *J. Environ. Nanotechnol.*, 9(1), 50–59 (2022). https://doi.org/10.13074/jent.2021.03.201394

Vidal, J., Vigil, O., de, M. O., López, N., Zelaya, A. O., Influence of NH3 concentration and annealing in the properties of chemical bath deposited ZnS films, *Mater. Chem. Phys.*, 61(2), 139–142 (1999). https://doi.org/10.1016/S0254-0584(99)00130-3

Wu, Q., Lu, D., Kumar, K. K., Ho, W., Cao, D., Zeng, Y., Zhang, B., Zhang, Y., Xie, L., Zhao, B., Wang, Z., Hao, H., Fan, H. and Wang, H., Highly efficient photocatalytic degradation for antibiotics and mechanism insight for Bi2S3/g-C3N4 with fast interfacial charges transfer and excellent stability, *Arab. J. Chem.*, 15(3), 103689 (2022). https://doi.org/ 10.1016/j.arabjc.2022.103689

Xu, Y., Liu, J., Xie, M., Jing, L., Yan, J., Deng, J., Xu, H., Li, H. and Xie, J., Graphene oxide-modified LaVO 4 nanocomposites with enhanced photocatalytic degradation efficiency of antibiotics, *Inorg. Chem. Front.*, 5(11), 2818–2828 (2018). https://doi.org/10.1039/C8QI00864G

Yu, F. P., Ou, S. L., Yao, P. C., Wu, B. R., Wuu, D. S., Structural, Surface Morphology and Optical Properties of ZnS Films by Chemical Bath Deposition at Various Zn/S Molar Ratios, *J. Nanomater.*, 2014, 1–7 (2014). https://doi.org/ 10.1155/2014/594952

Yuan, X., Hua, J., Zeng, R., Zhu, D., Ji, W., Jing, P., Meng, X., Zhao, J. and Li, H., Efficient white light emitting diodes based on Cu-doped ZnInS/ZnS core/shell quantum dots, *Nanotechnol.*, 25(43), 435202 (2014). https://doi.org/10.1088/0957-4484/25/43/435202